# Monostatic and Bistatic Polarimetric Observations of Snow Cover on Top of the Great Aletsch Glacier at Ku-band


**Marcel Stefko**[1], Philipp Bernhard[1], Othmar Frey[1,2], Irena Hajnsek[1,3]

[1]Chair of Earth Observation and Remote Sensing, ETH Zürich
[2]GAMMA Remote Sensing
[3]Microwaves and Radar Institute, German Aerospace Center DLR



POLINSAR workshop, 22nd June 2023


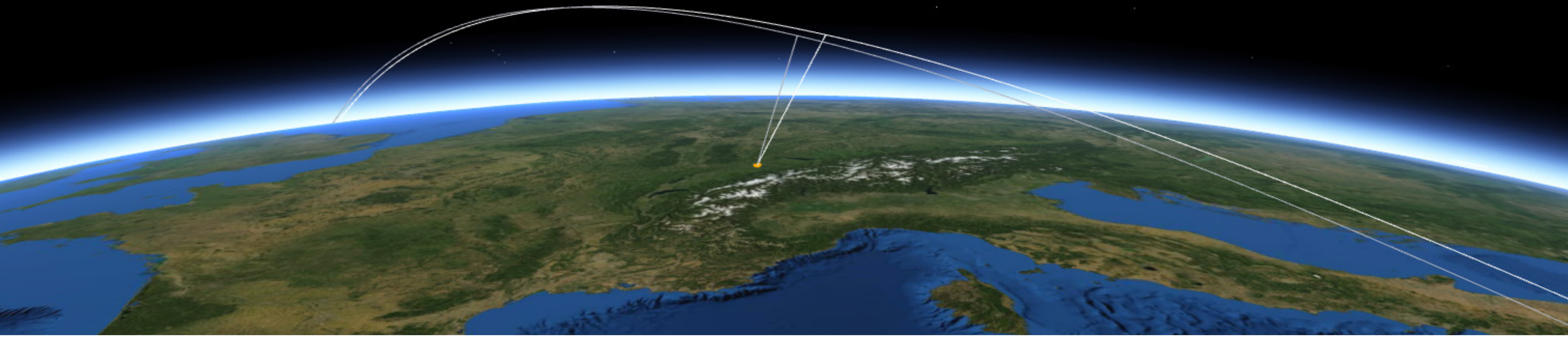

Earth Observation and Remote Sensing

ETH zürich

# Motivation

- Spaceborne radar observation missions are extremely powerful tools for global monitoring of natural environments.
- They are however expensive to develop and operate, and require extensive proof-of-concept and validation data, before they are accepted.
- Low availability of reference experimental data (and instruments) hinders the conceptualization, development and validation of new spaceborne mission concepts, especially in less conventionally used configurations (e.g. bistatic radar, full-polarimetric radar, or in less popular frequency bands).
- Ground-based systems are a cost-efficient way to explore novel concepts and gain insights into scattering properties of natural media at less-used configurations (e.g. Ku-band).

# Bistatic operation mode of KAPRI

- Two KAPRI devices work in tandem:
  - Primary (P) transmitter-receiver (monostatic)
  - Secondary (S) receiver (bistatic)
- Direct synchronization link is established between devices to correct oscillator offsets.

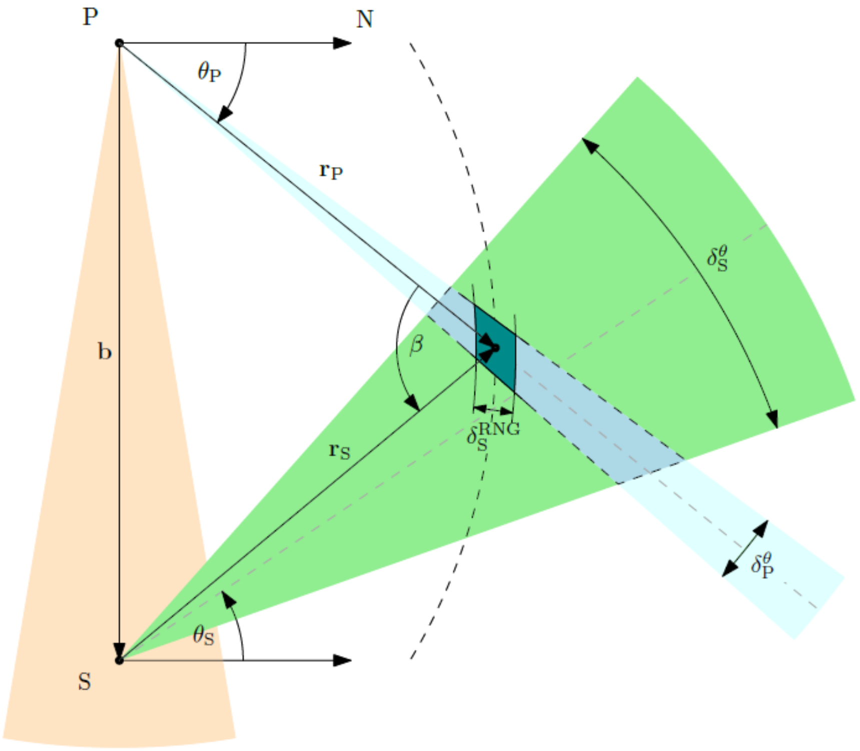


| Parameter | Symbol | Value |
|---|---|---|
| Start frequency | $f_c$ | 17.1 GHz |
| Chirp bandwidth | $B$ | up to 200 MHz |
| Output power | $P_t$ | 21.5 dBm |
| Receiver noise figure | $F_n$ | 3.1 dB at 290 K |
| FMCW chirp duration | $\tau$ | between 250 µs and 16 ms |
| Range sample spacing | $\delta^{rs}$ | 0.75 m |
| Primary (P) azimuth beamwidth | $\delta_P^\theta$ | 0.5° |
| Primary (P) elevation beamwidth | $\delta_P^\varepsilon$ | >31° |
| Secondary (S) azimuth beamwidth | $\delta_S^\theta$ | 12° |
| Secondary (S) elevation beamwidth | $\delta_S^\varepsilon$ | 24° |
| Clock frequency | $f_{clock}$ | 100 MHz GPS-disciplined |

*Note: Beamwidth values correspond to one-way HPBW.*

# Great Aletsch Glacier observations

- Observations of the Jungfraufirn area of the Great Aletsch Glacier
- 2 seasons:
  - Late summer (Aug 2021)
  - Late winter (Mar 2022)
- Radar measurements:
  - Polarimetric
  - Interferometric
  - Bistatic
- In-situ measurements:
  - Snow grain size
  - Snow density
  - Snow temperature

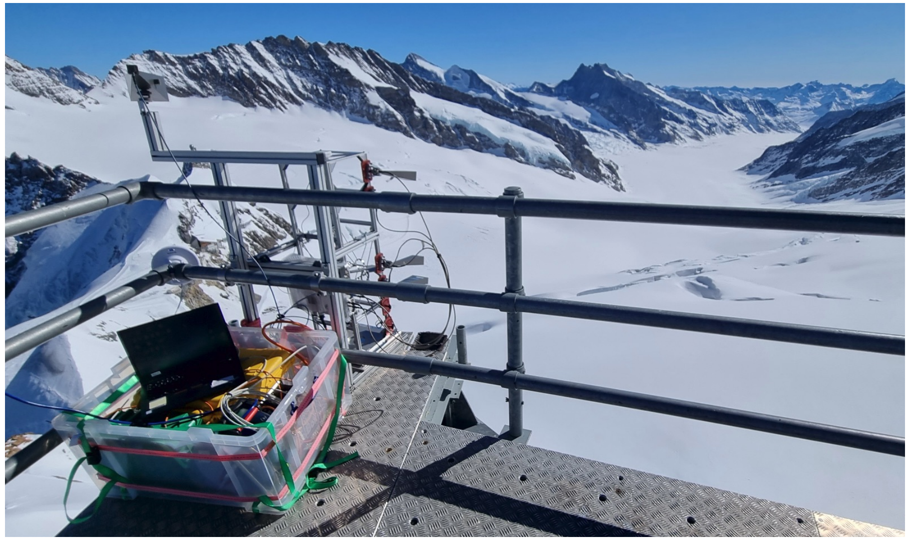

# Bistatic KAPRI operation

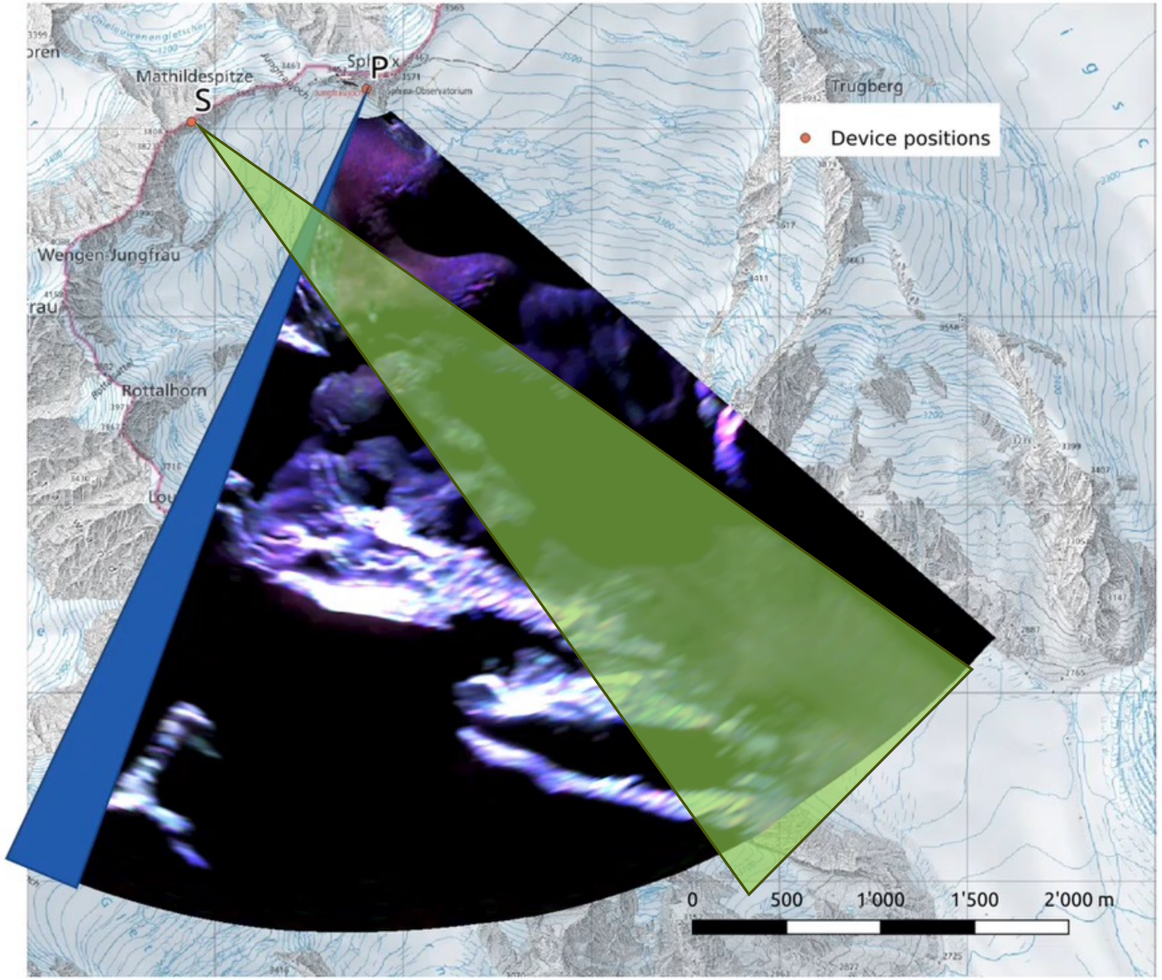


The primary KAPRI device performs an azimuthal scan with the real-aperture antennas, acquiring a monostatic dataset.
The secondary KAPRI device is deployed in receive-only mode in a different location to acquire a bistatic dataset.

# Monostatic polarimetric observations – Pauli RGB images

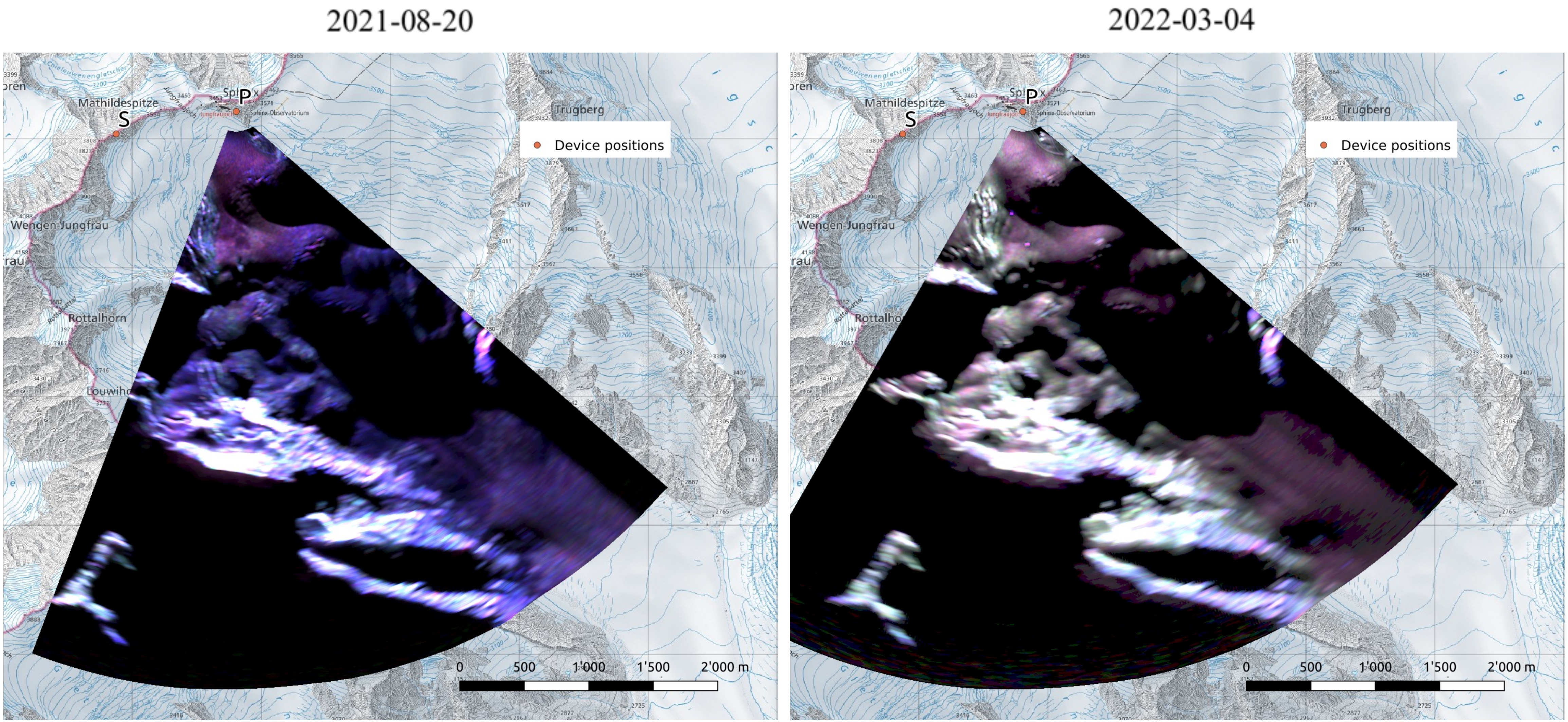


**HH+VV** **HH-VV** **HV+VH**

# Bistatic polarimetric observations – Pauli RGB images

2021-08-20

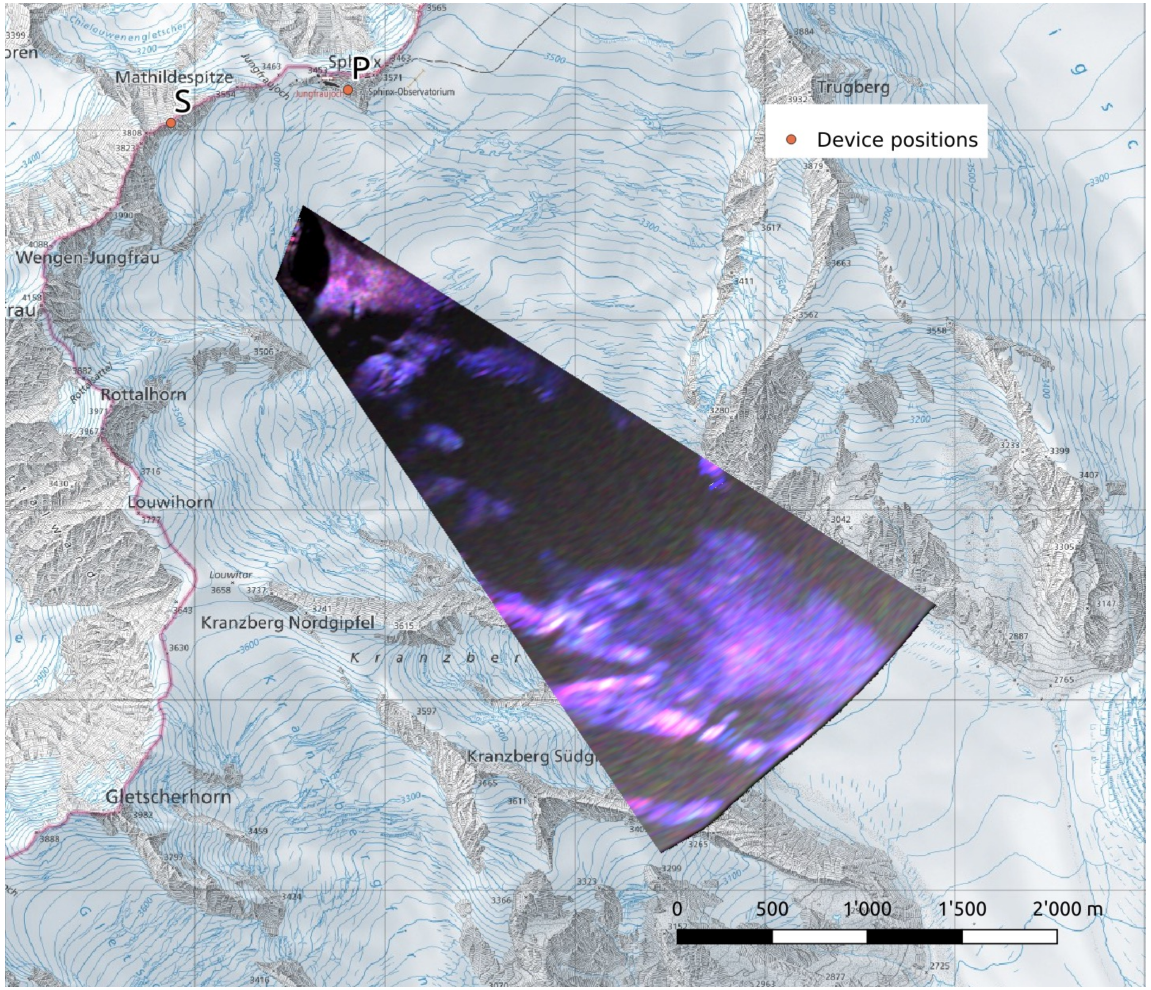


2022-03-04

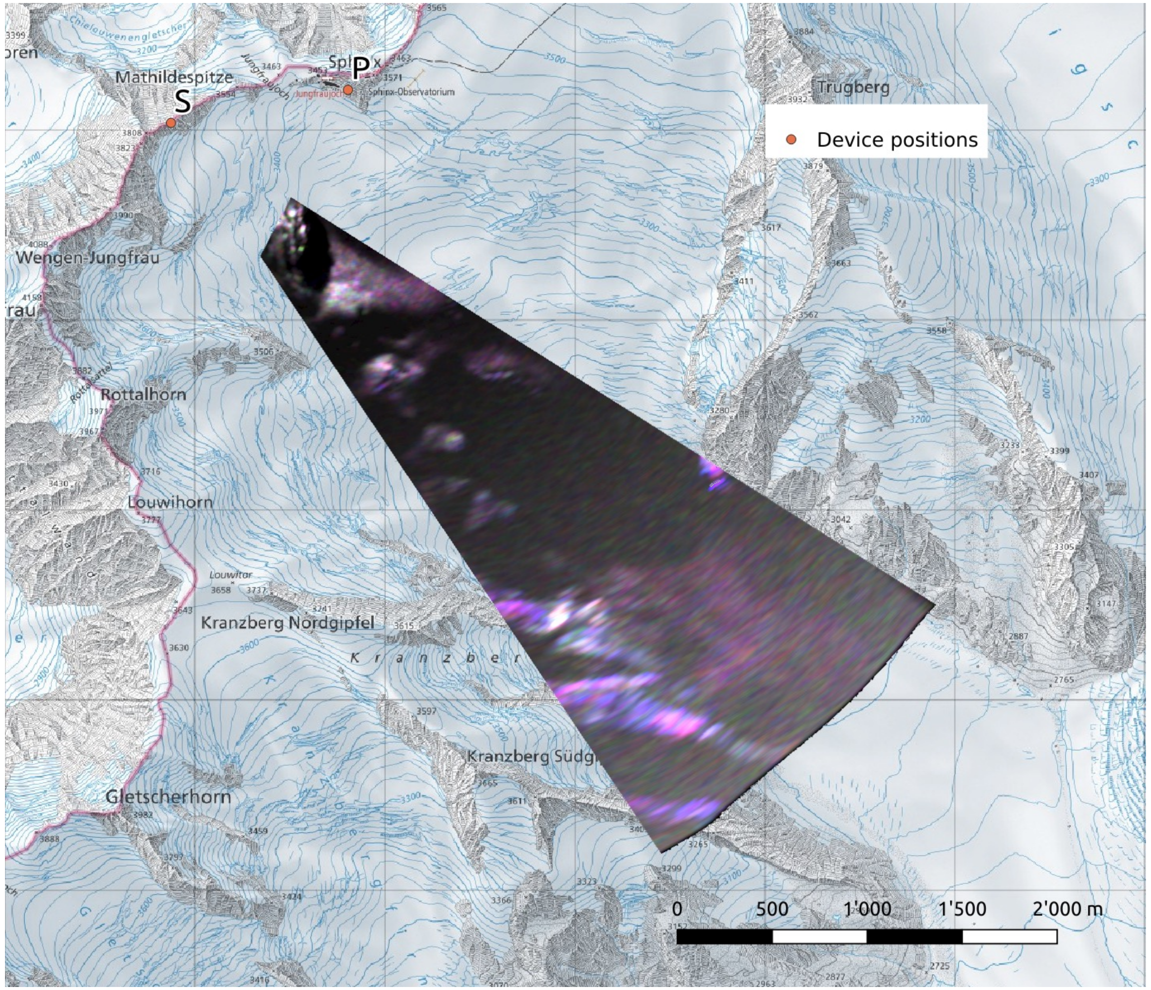


**HH+VV** **HH-VV** **HV+VH**

# (Selected) radar observables of snow and ice

- Temporal coherence $\gamma \in [0,1]$
  - quantifies temporal stability of scatterers within the scene,
  - is important for repeat-pass methods.
- Entropy $H \in [0,1]$, mean alpha angle $\bar{\alpha} \in [0°, 90°]$
  - diversity and average "type" of scattering process
- Co-polar phase difference (CPD): $\phi_{CPD} = \phi_{HH} - \phi_{VV} \in [-180°, 180°]$
  - indicates anisotropy of snow structure,
  - analyzed in literature (e.g. Leinss et al. 2016, Parrella et al. 2021).
- Cross-polar phase difference (XPD): $\phi_{XPD} = \phi_{HV} - \phi_{VH} \in [-180°, 180°]$
  - can only have a non-zero value in bistatic acquisitions due to reciprocity principle,
  - is not as well theoretically explored as the CPD.

At Ku-band, the short wavelength causes the parameters to be in general very sensitive to small shifts and structural changes.

# Temporal view of temporal coherence

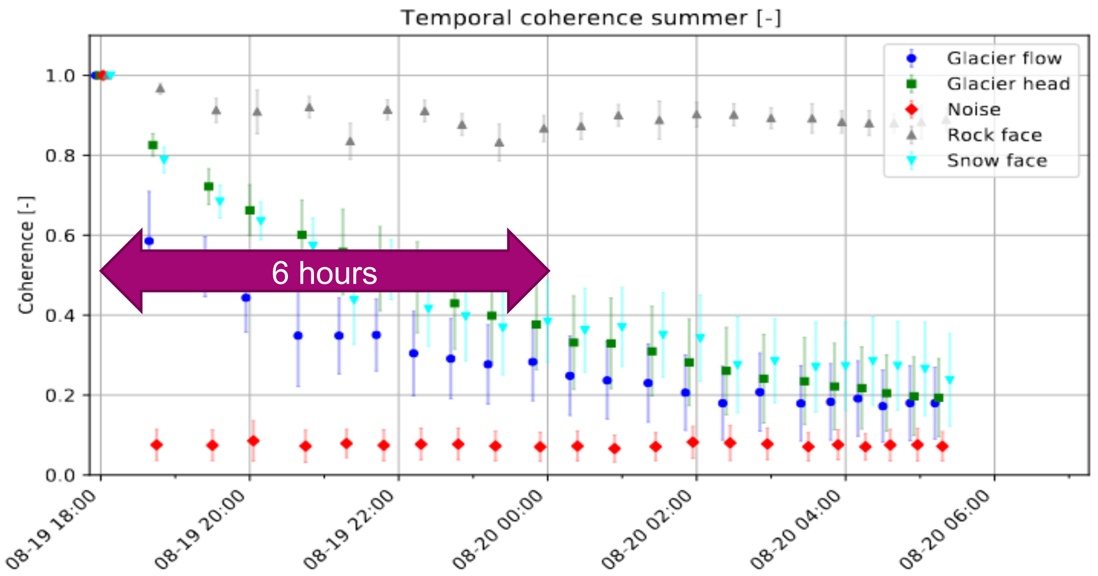


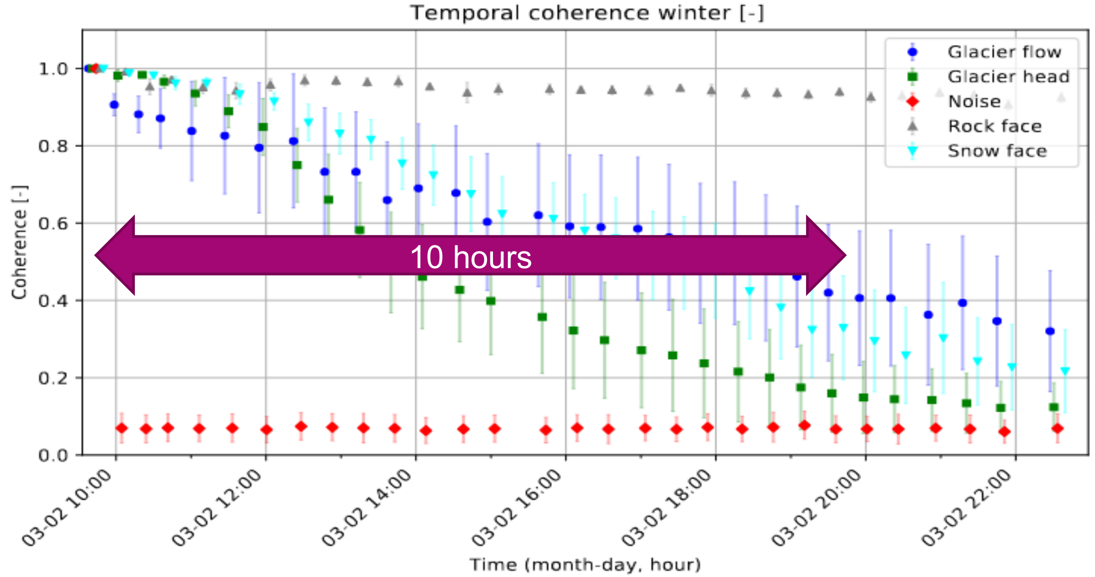


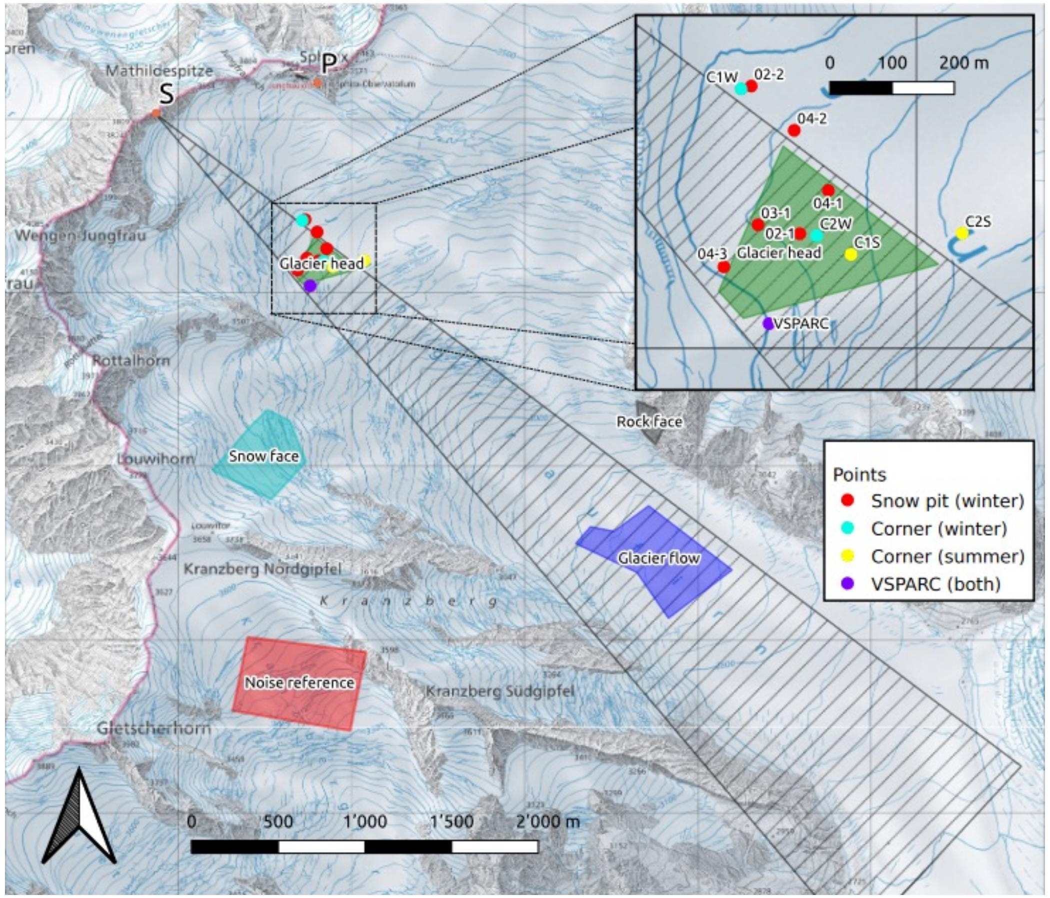


Coherence decay occurs on scales of 6 to 10 hours -> implications for satellite missions.

# Entropy $H$

2021-08-20

2022-03-04

Morning

Evening

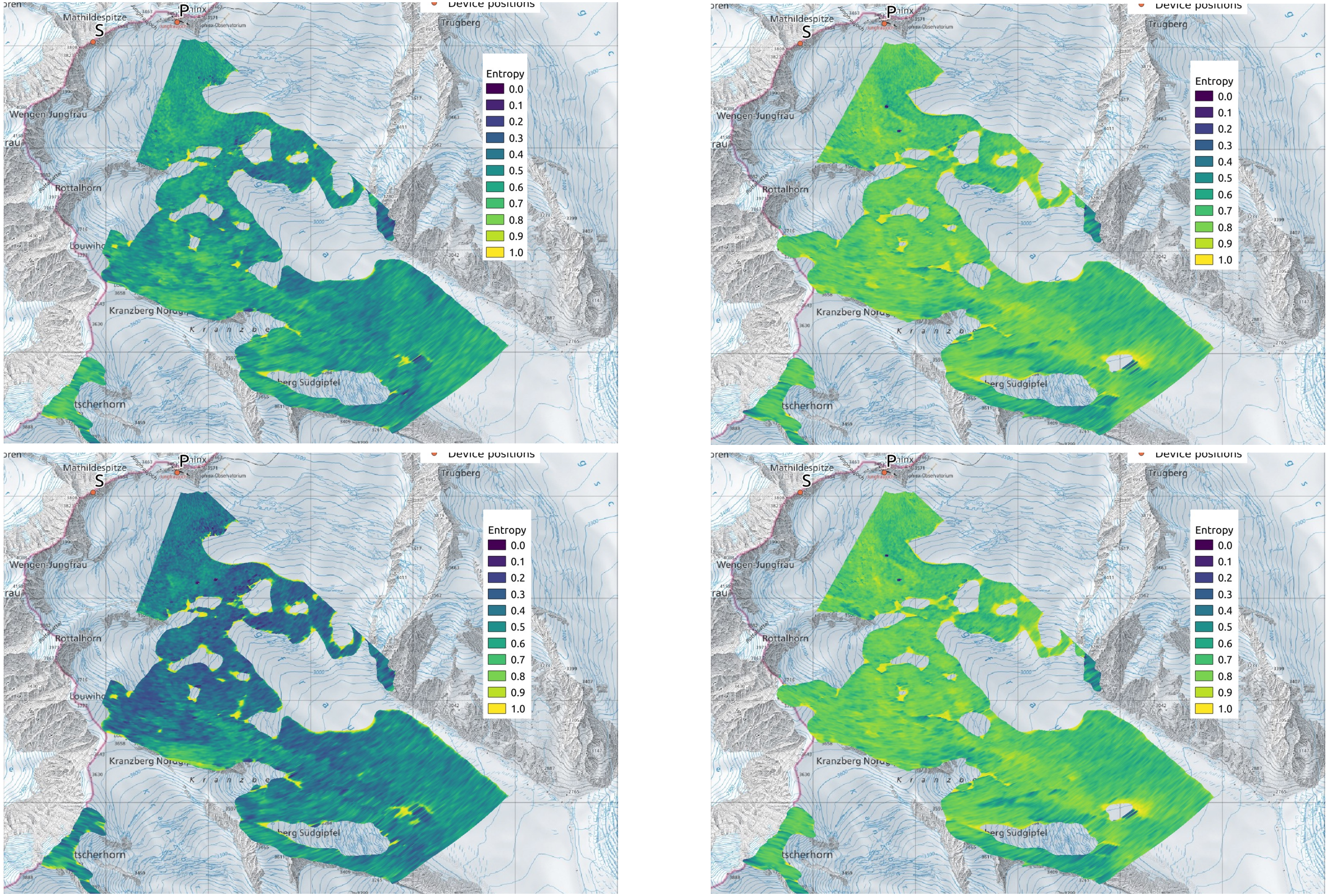

# Mean alpha angle $\bar{\alpha}$

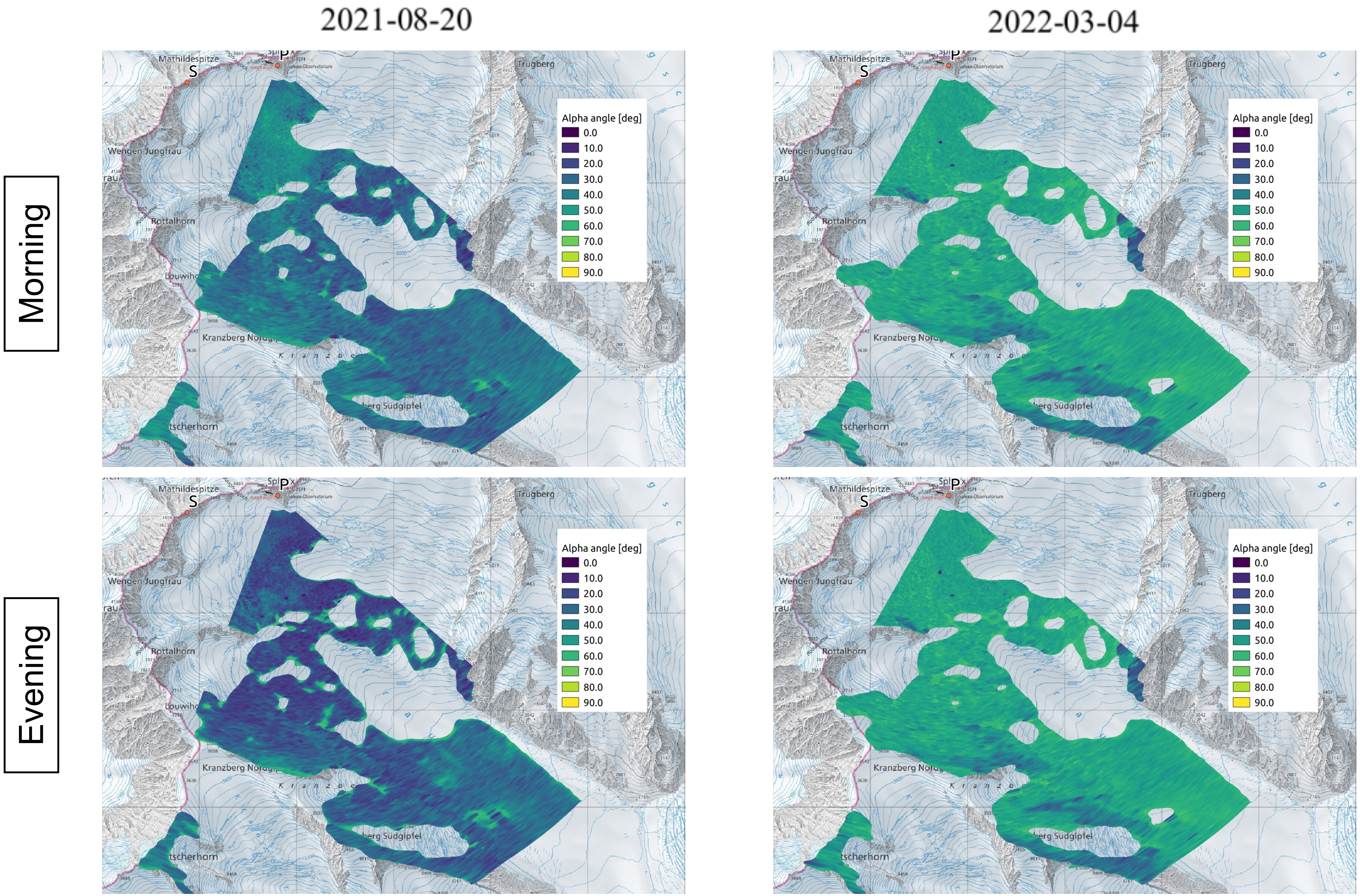

# Monostatic CPD

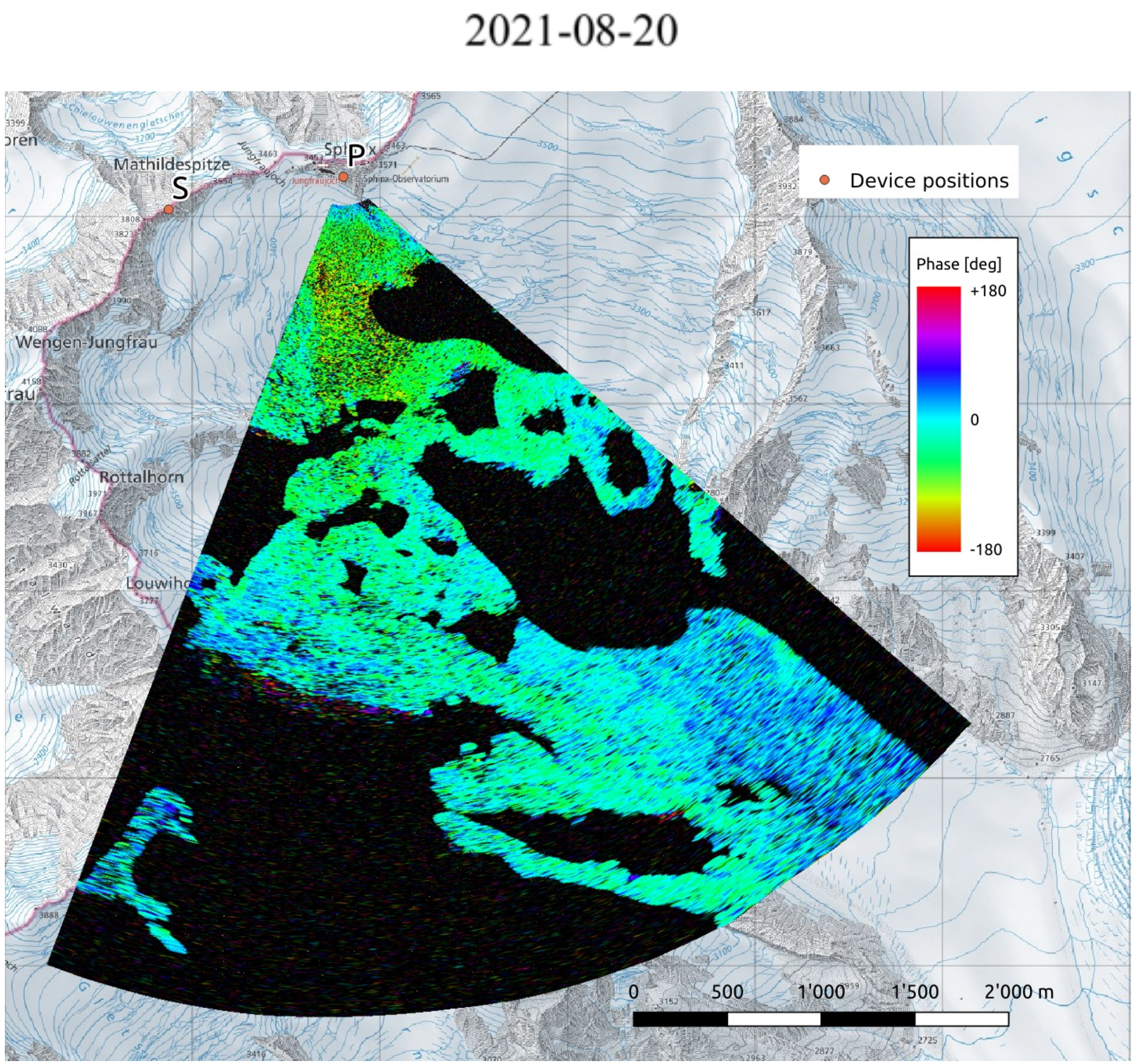


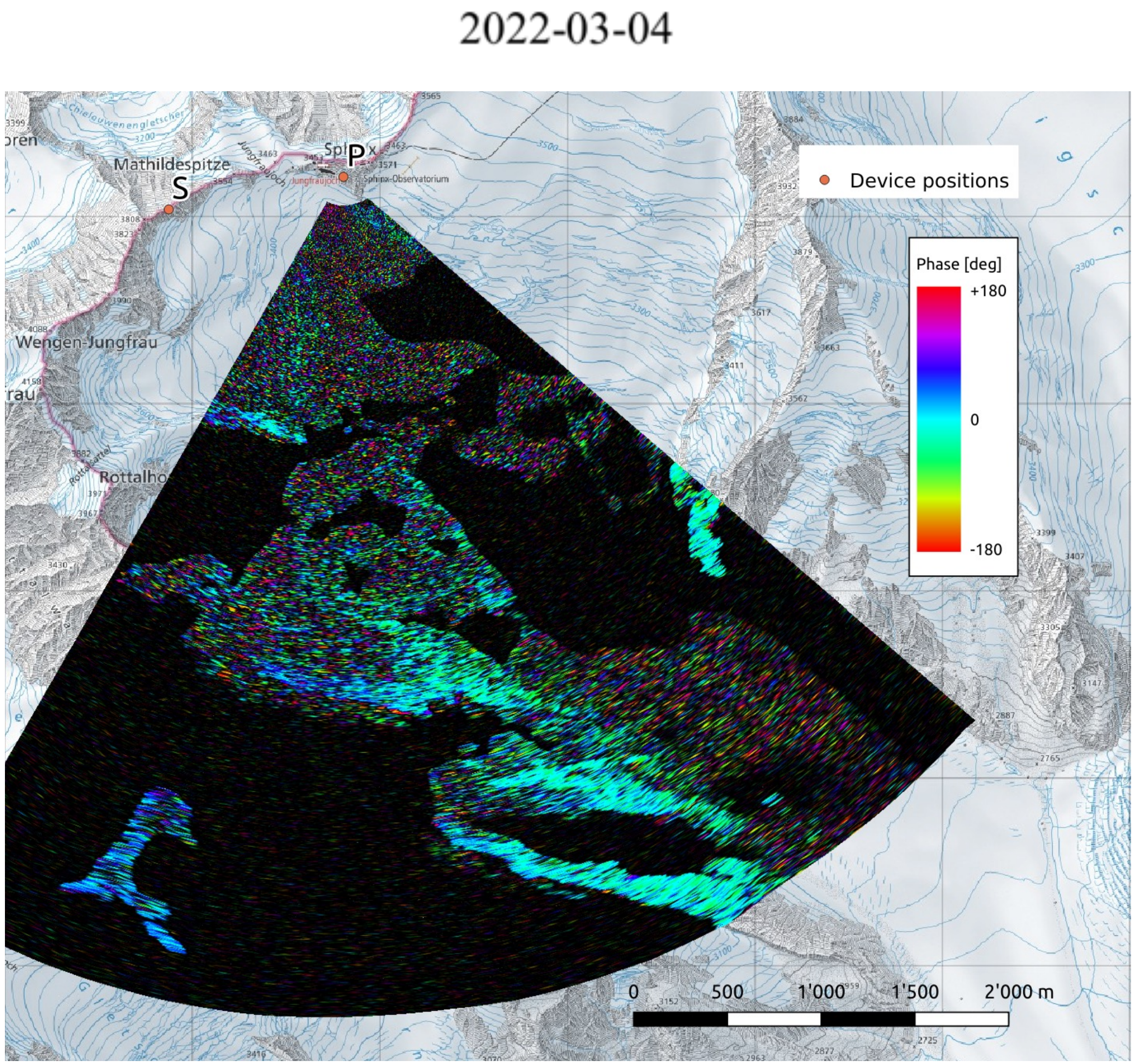

# Bistatic CPD

2021-08-20

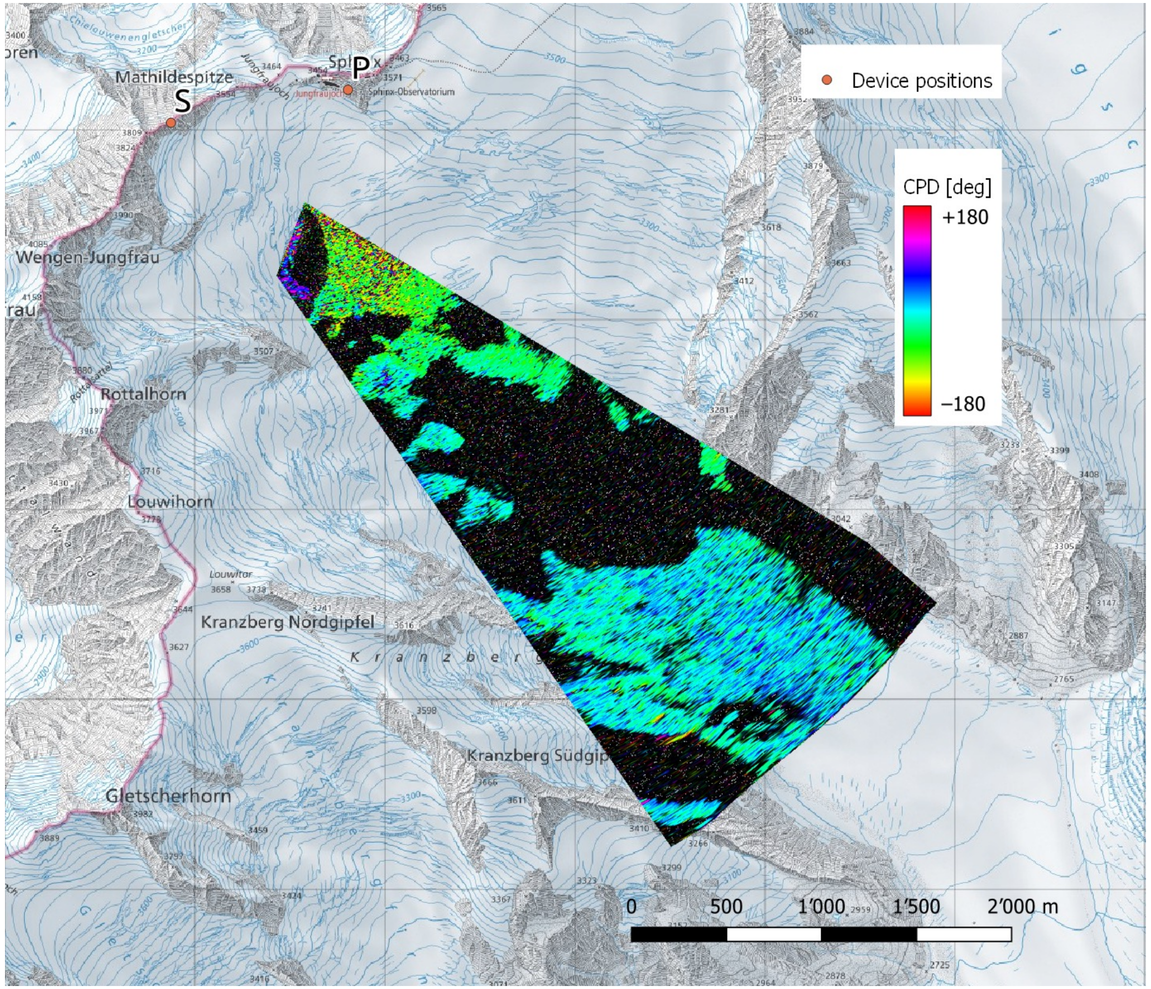


2022-03-04

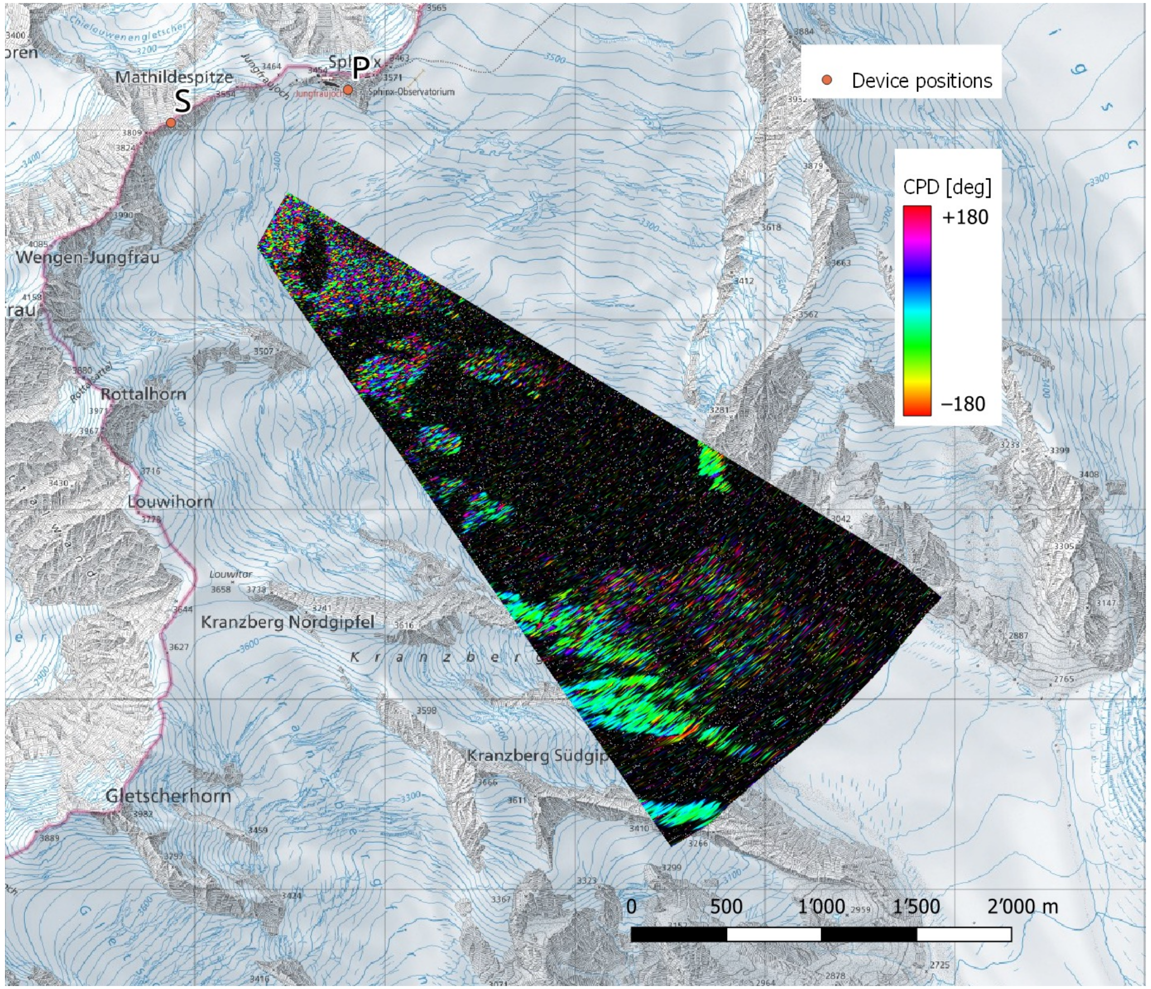

# Monostatic XPD

2021-08-20

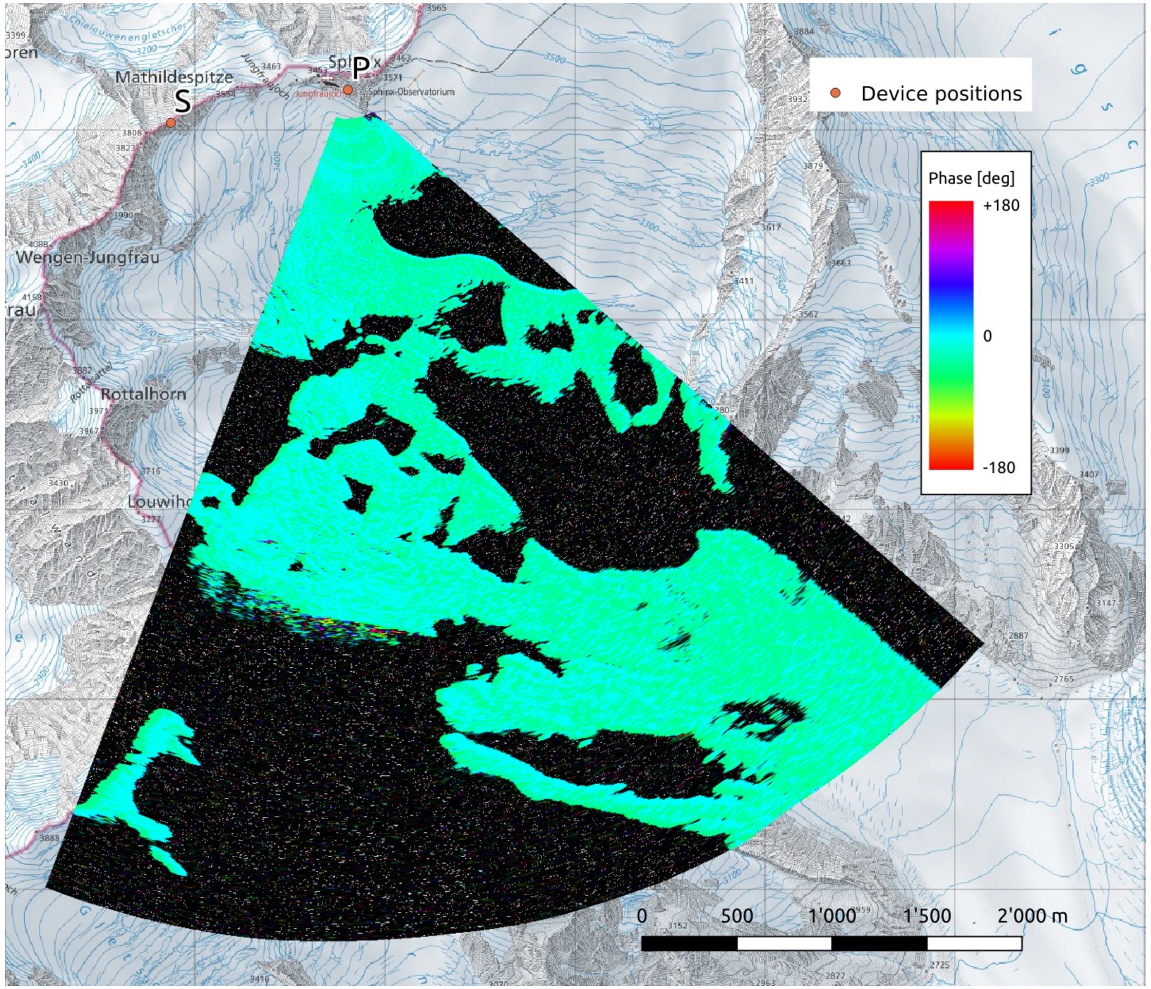


2022-03-04

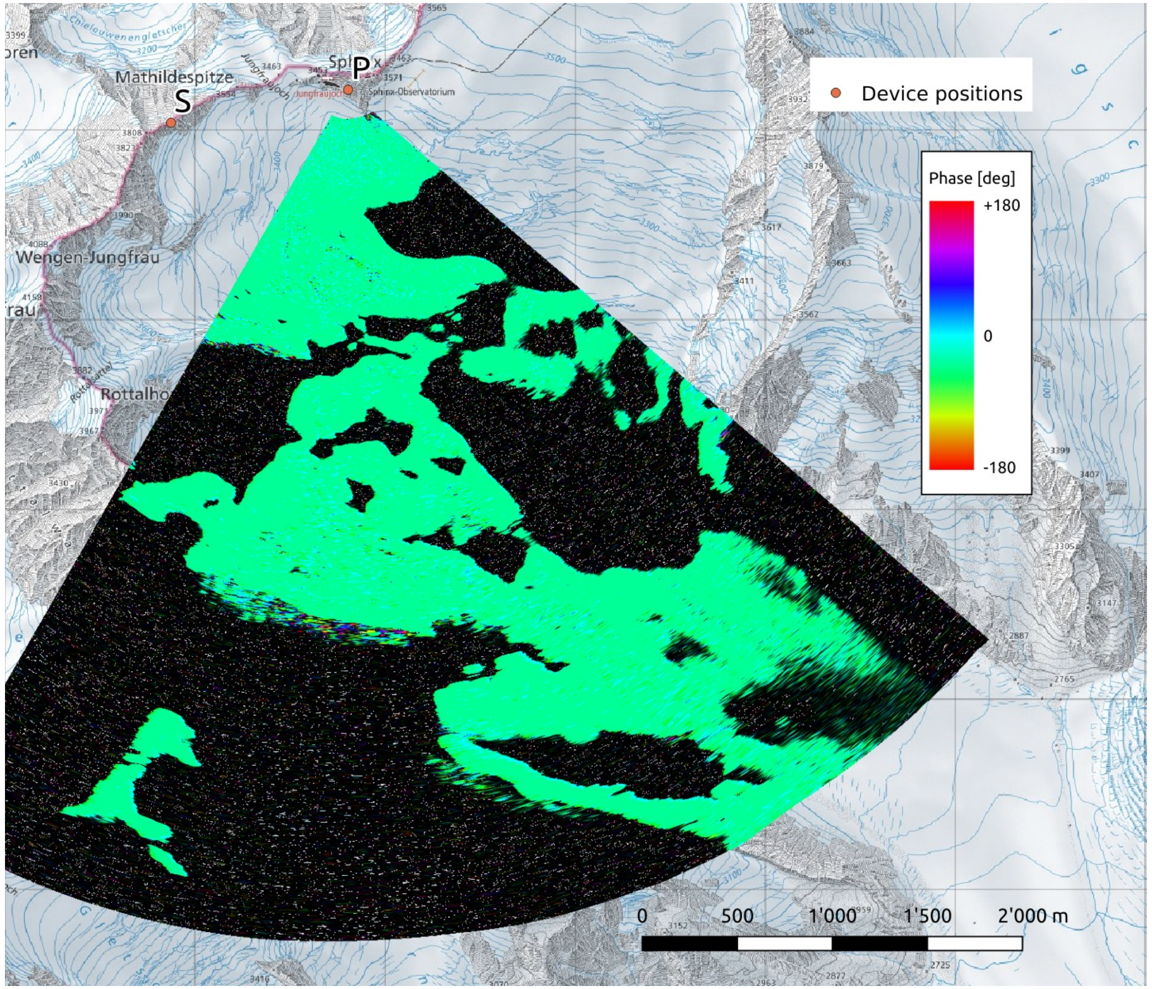

# Bistatic XPD

2021-08-20

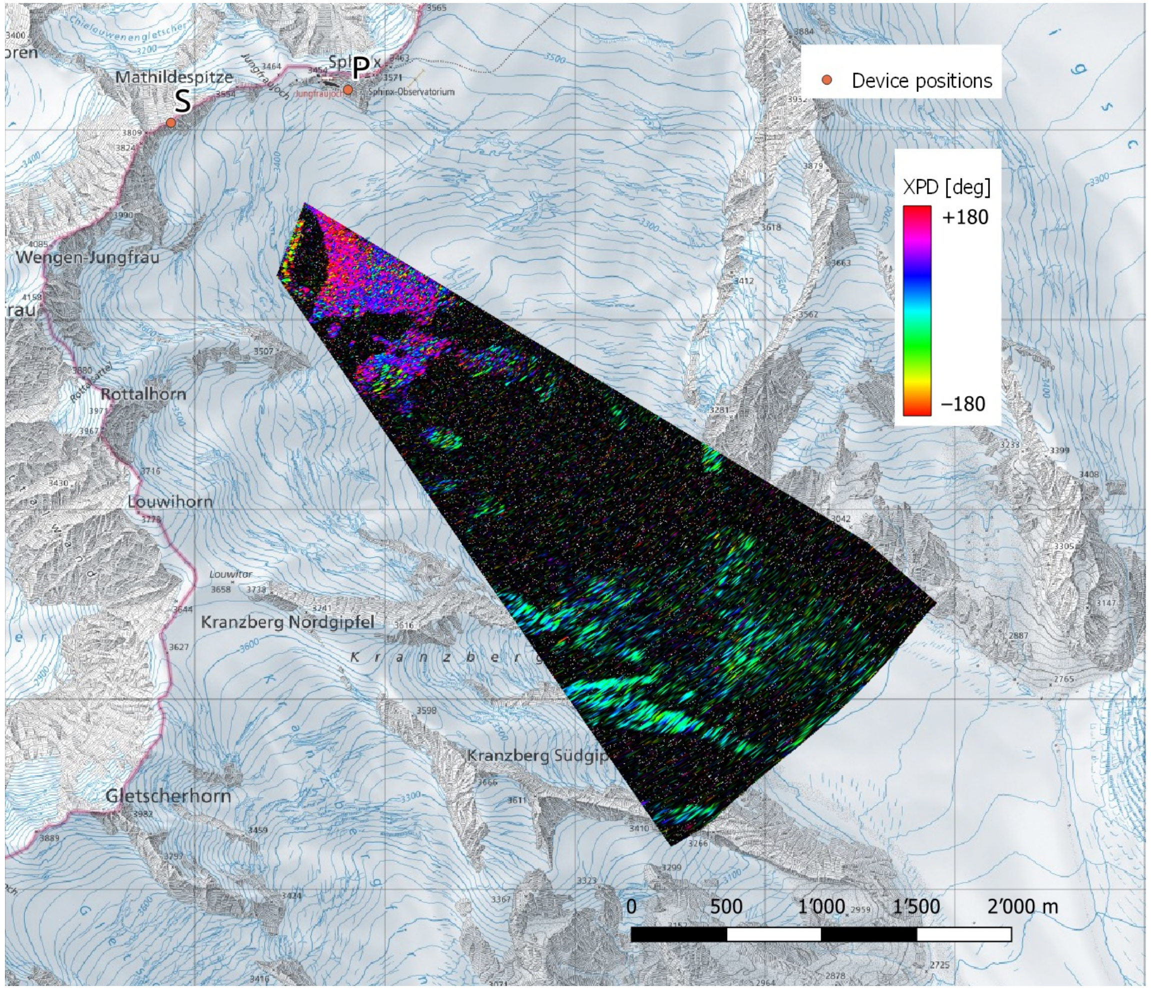


2022-03-04

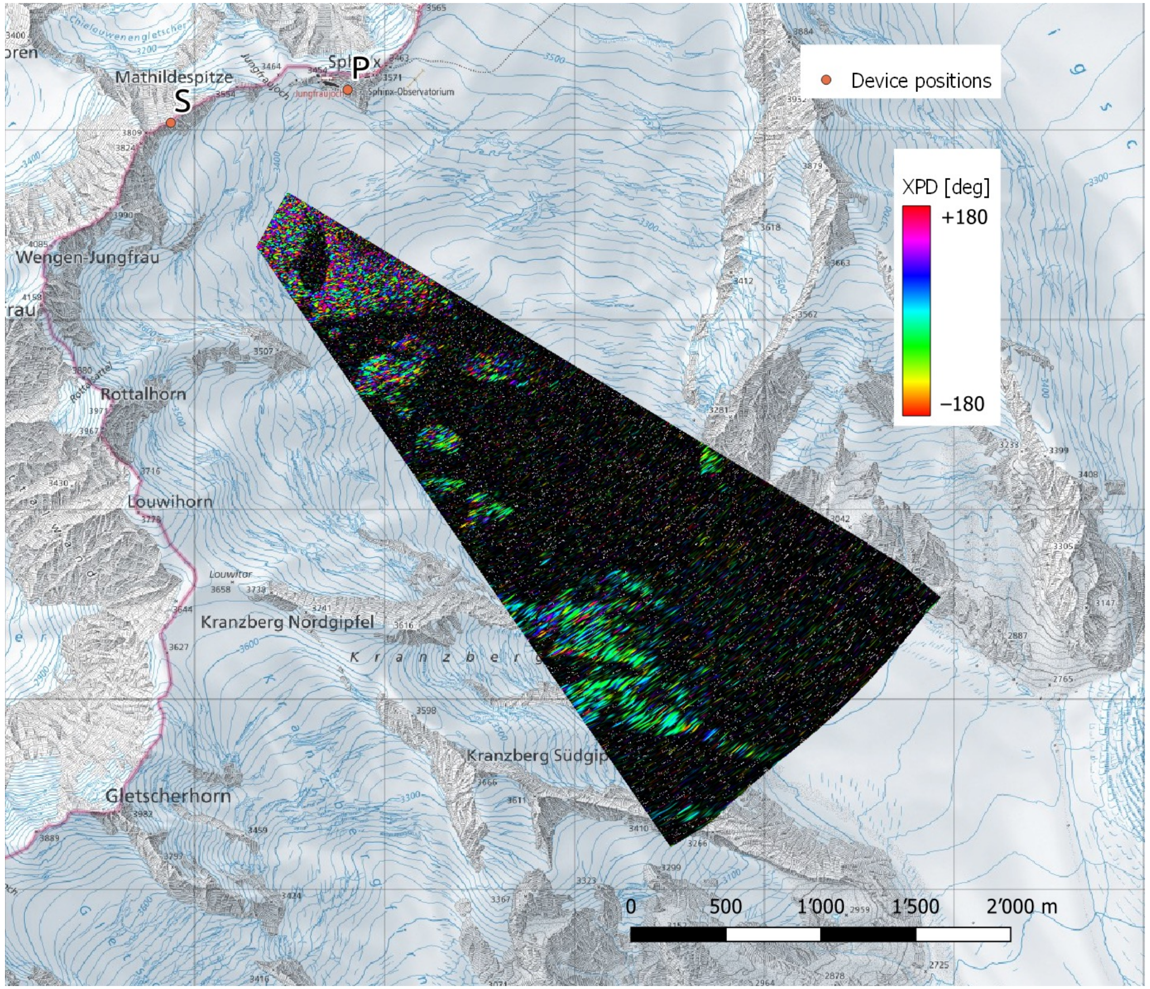

# Conclusions

- **Polarimetric properties vary dramatically between summer and winter.**
- **Phase differences at Ku-band are prone to phase-wrapping when a thick layer of seasonal snow is present – parameter inversion may be difficult.**
- **Non-zero XPD value observed in bistatic regime – the reciprocity principle cannot be assumed.**
- **Snow cover at Ku-band decorrelates within 6-10 hours → implications for repeat pass radar imaging methods.**
- **Lessons learned can help provide better prior estimates of parameters for future observation missions.**

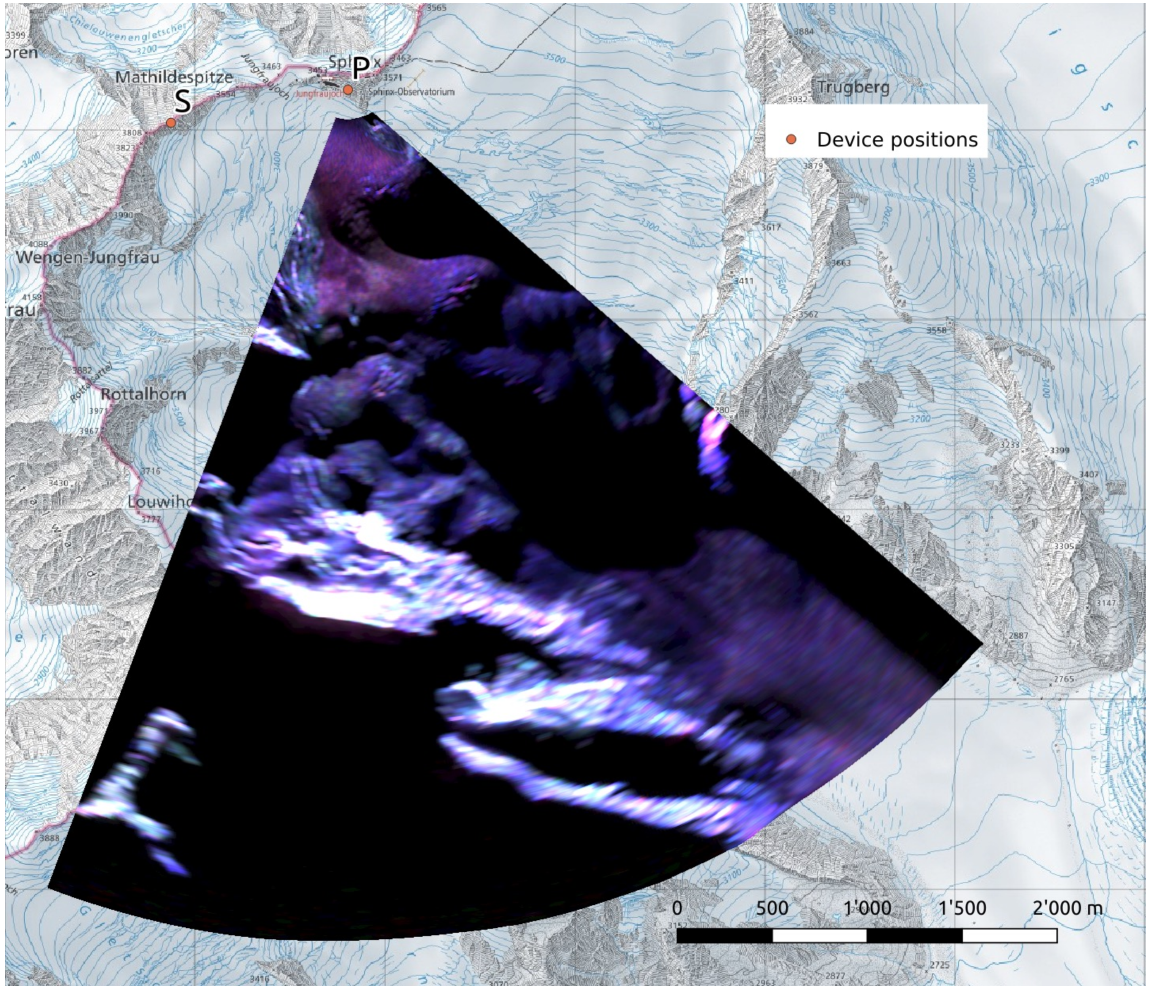


See also: Stefko et al., "Polarimetric analysis of bi-seasonal monostatic and bistatic radar observations of a glacier accumulation zone at Ku-band," IEEE JSTARS, 2023, in review.

# Coming soon @ EO ETH @ Jungfraujoch

- Deeper analysis of interferometric data – see also poster #167 by Esther Mas i Sanz.
- Enhancement of polarimetric data – temporal averaging to boost signal, temporal analysis.
- Investigation of coherent backscatter opposition effect (CBOE).

# Any questions?

# BACKUP SLIDES

# Cross polar phase difference $\phi_{HV-VH}$ (XPD)

- Cross-polarized channels:
  - HV: Transmitted vertically, received horizontally
  - VH: Transmitted horizontally, received vertically
- $\phi_{HV-VH}$ quantifies the propagation path length difference between the HV and VH channels.
- In monostatic case, $\phi_{HV-VH}$ is always equal to zero.
- Due to this, XPD has not been as thoroughly theoretically explored as other parameters.
- In the bistatic case, its value can be non-zero and could provide insights into structure of the observed environment.

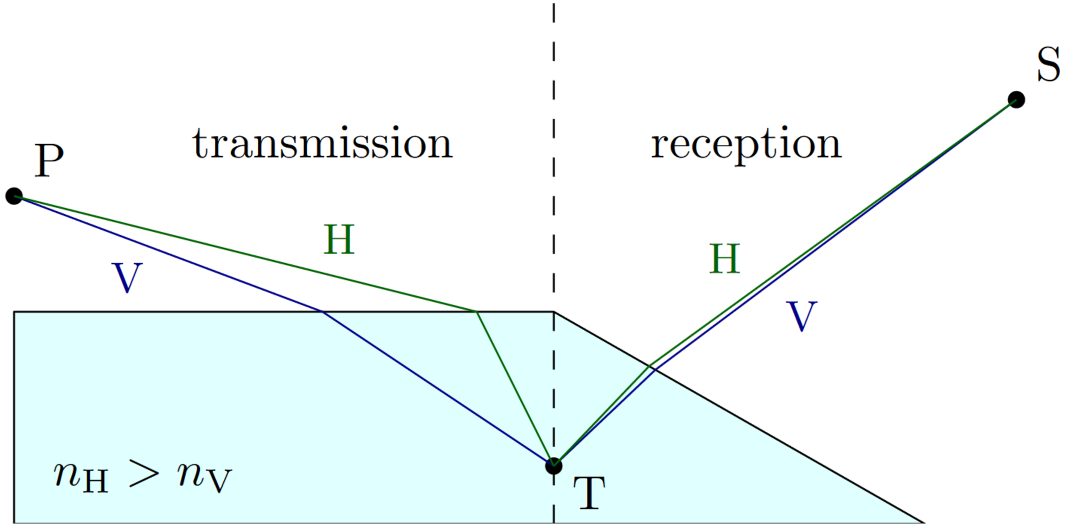

# Monostatic CPD (evening)

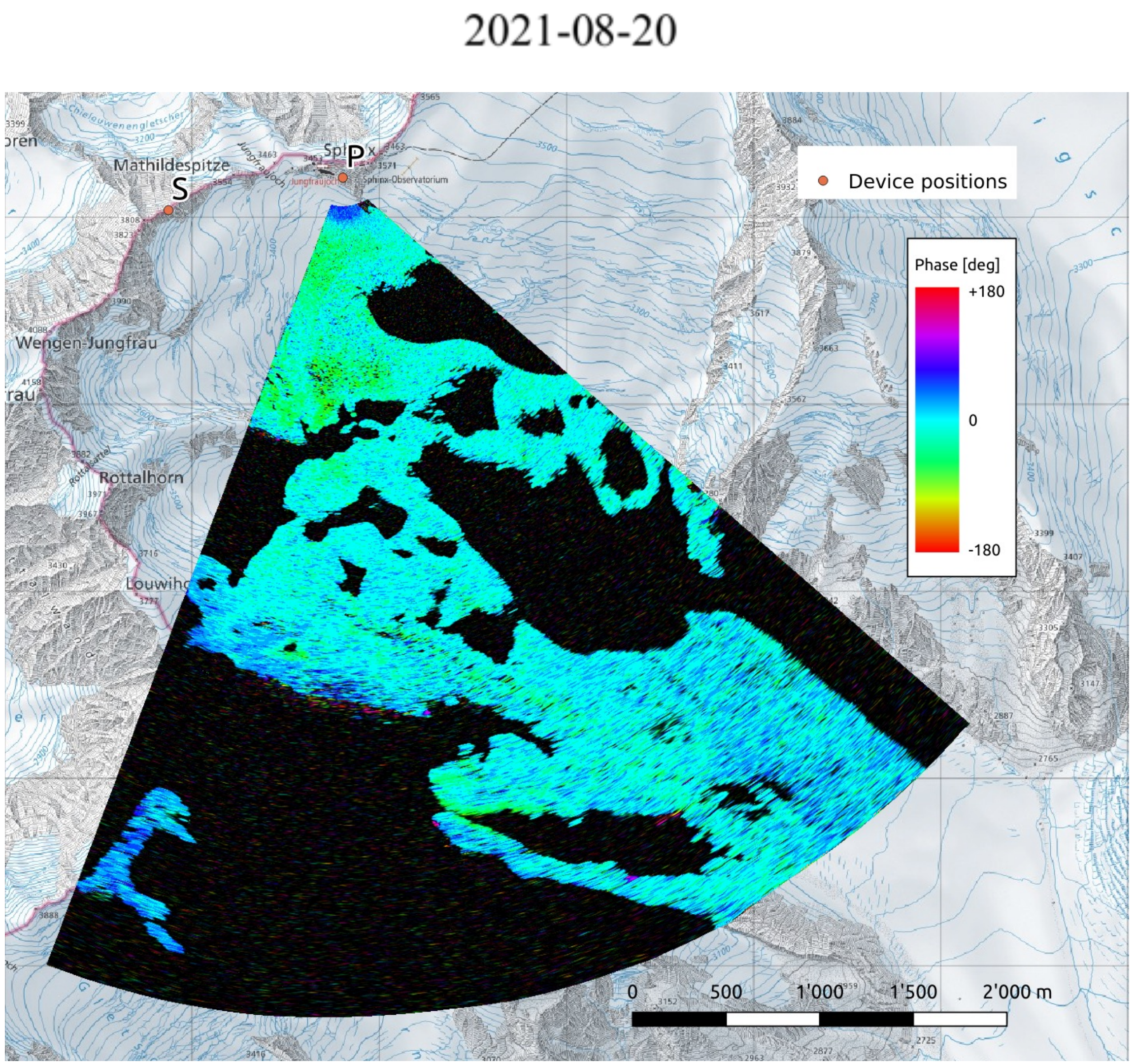


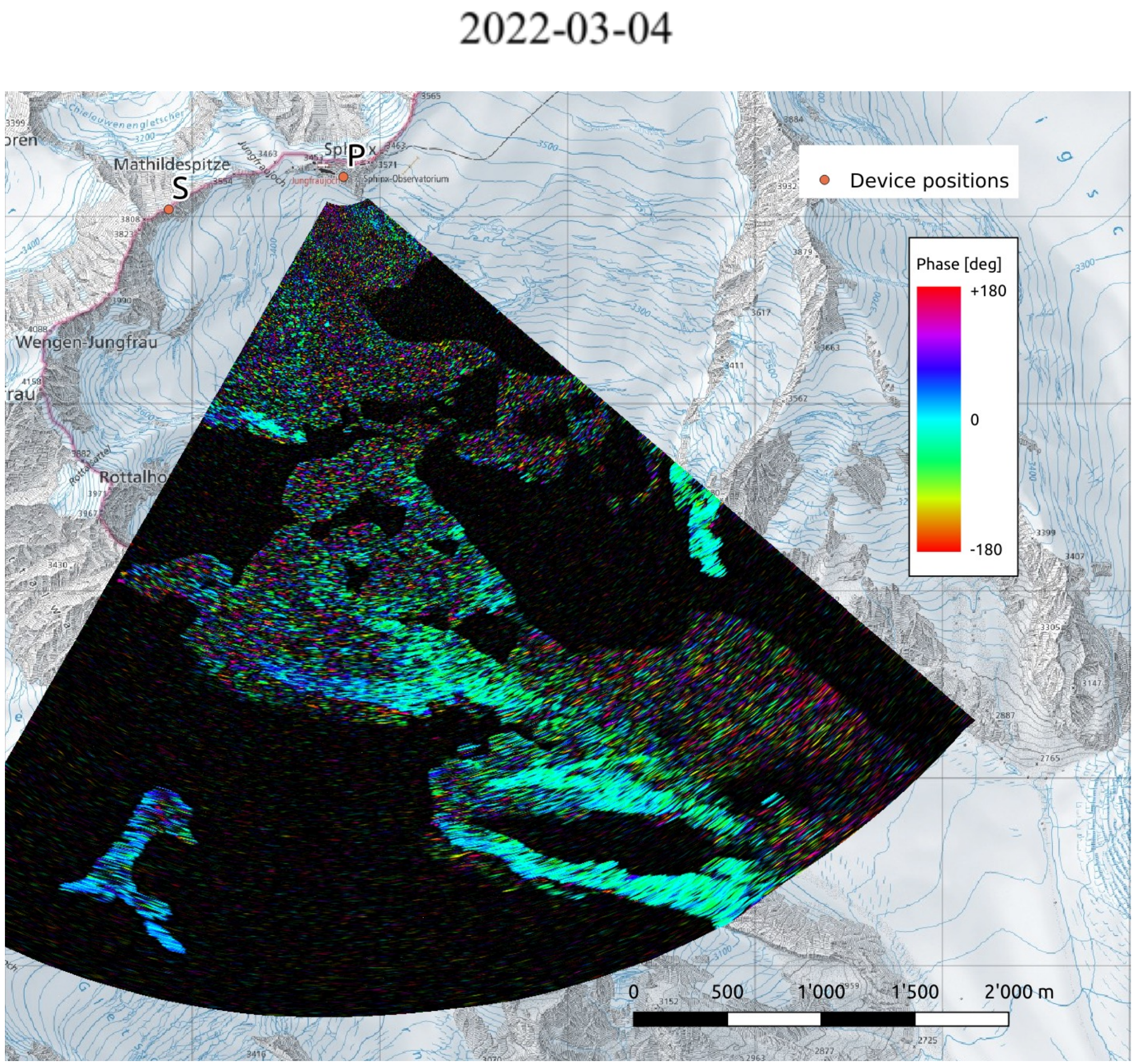

# Coherent Backscatter Opposition Effect (CBOE)

- Can be observed as a narrow spike of intensity around the monostatic backscatter direction ($\beta = 0$) in co-polarized channels.

- Occurrences:
  - Visible light: Particulate suspensions, cells of plants, lunar regolith (soil)
  - Radio waves: Lunar ice deposits, Mars' poles, Jupiter's moons
- Its occurrence had only recently been confirmed in terrestrial snow at radio wavelengths, mainly due to historical unavailability of bistatic data.

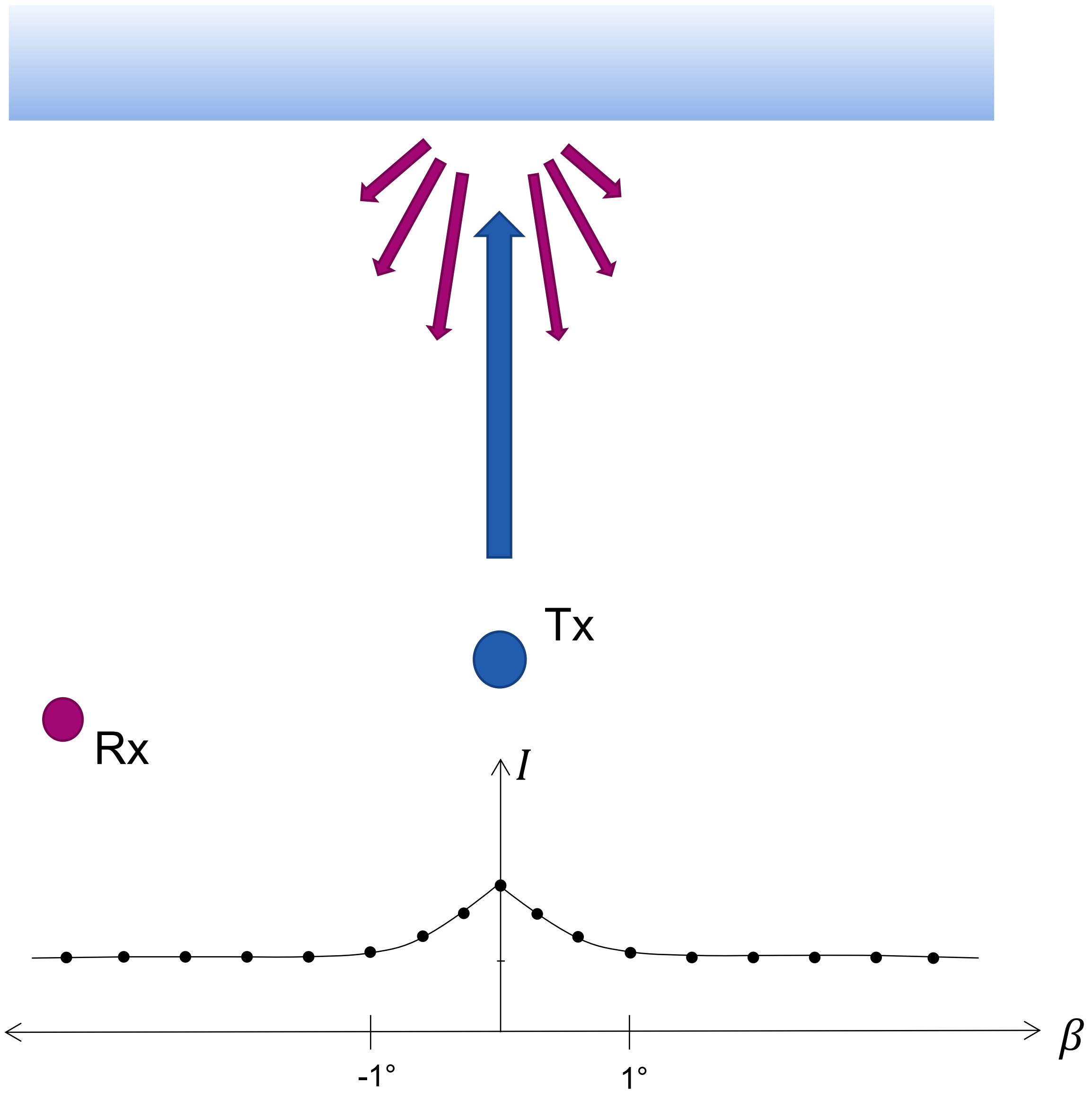

# Observation of the CBOE @ Ku-band

- KAPRI used for the first characterization of the full bistatic profile of the CBOE peak at Ku-band in the Earth's cryosphere, as a complement to TanDEM-X observations at X-band.
- Measurements of the peak shape can be used for parameter retrieval, e.g. scattering and absorption lengths.
- Further investigation needed – both theoretical and experimental.

KAPRI

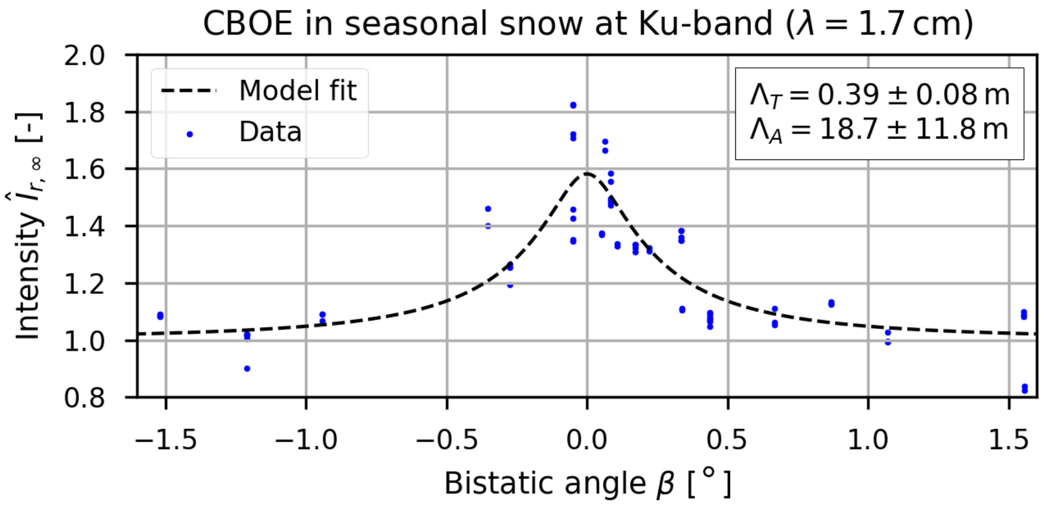


TanDEM-X

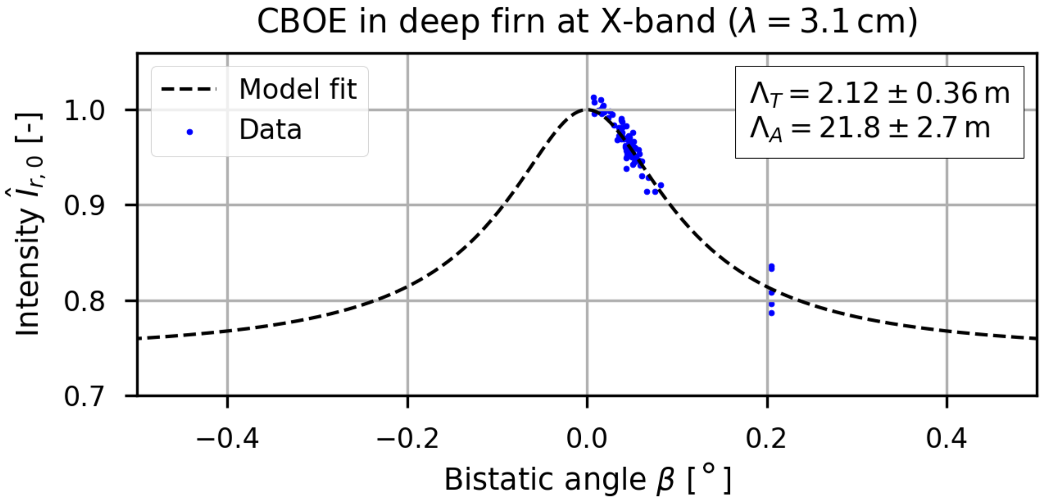



Stefko, M., Leinss, S., Frey, O., and Hajnsek, I.: Coherent backscatter enhancement in bistatic Ku- and X-band radar observations of dry snow (2022) The Cryosphere, 16, 2859–2879, https://doi.org/10.5194/tc-16-2859-2022

# Temporal coherence after 6 hours

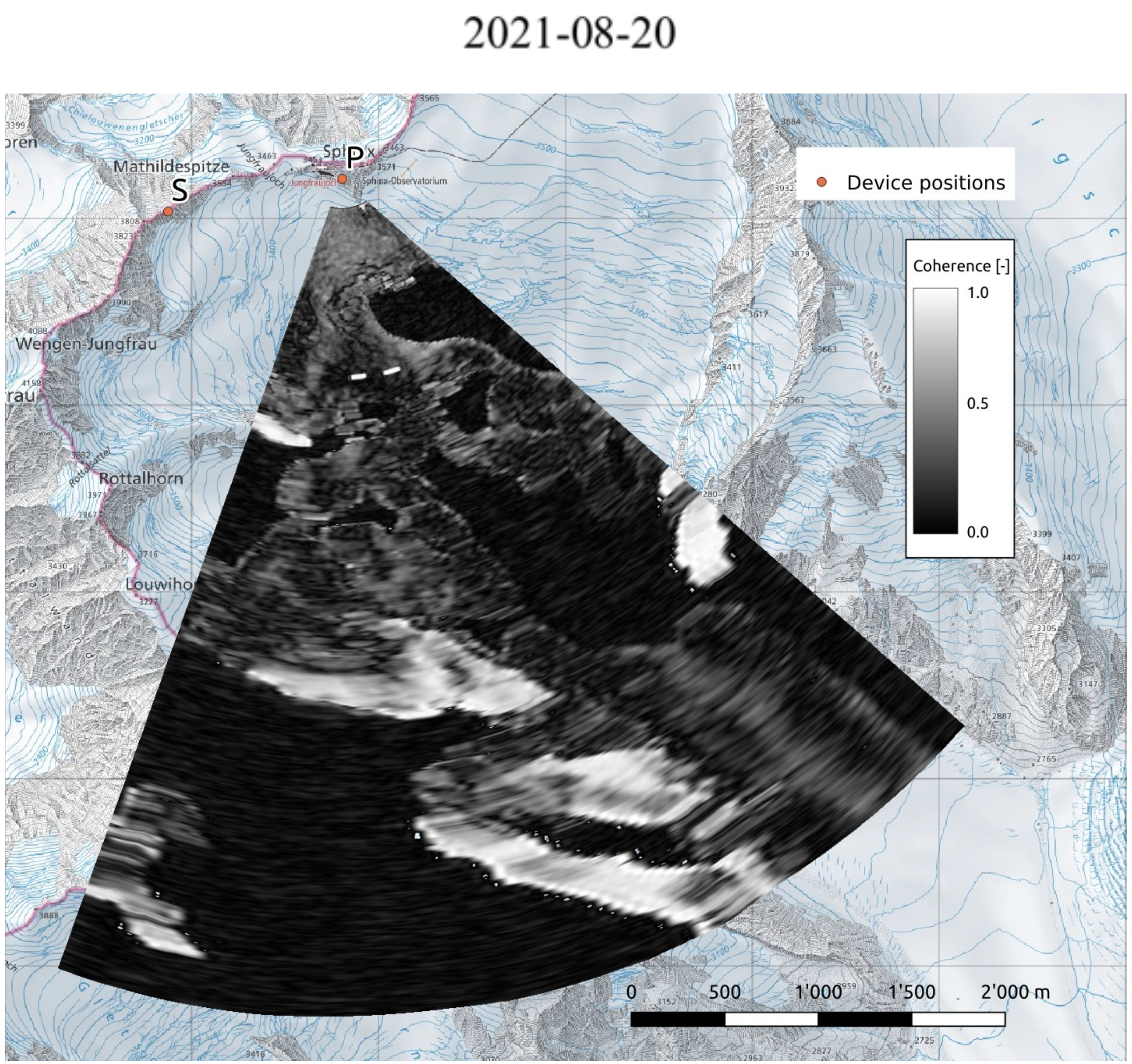


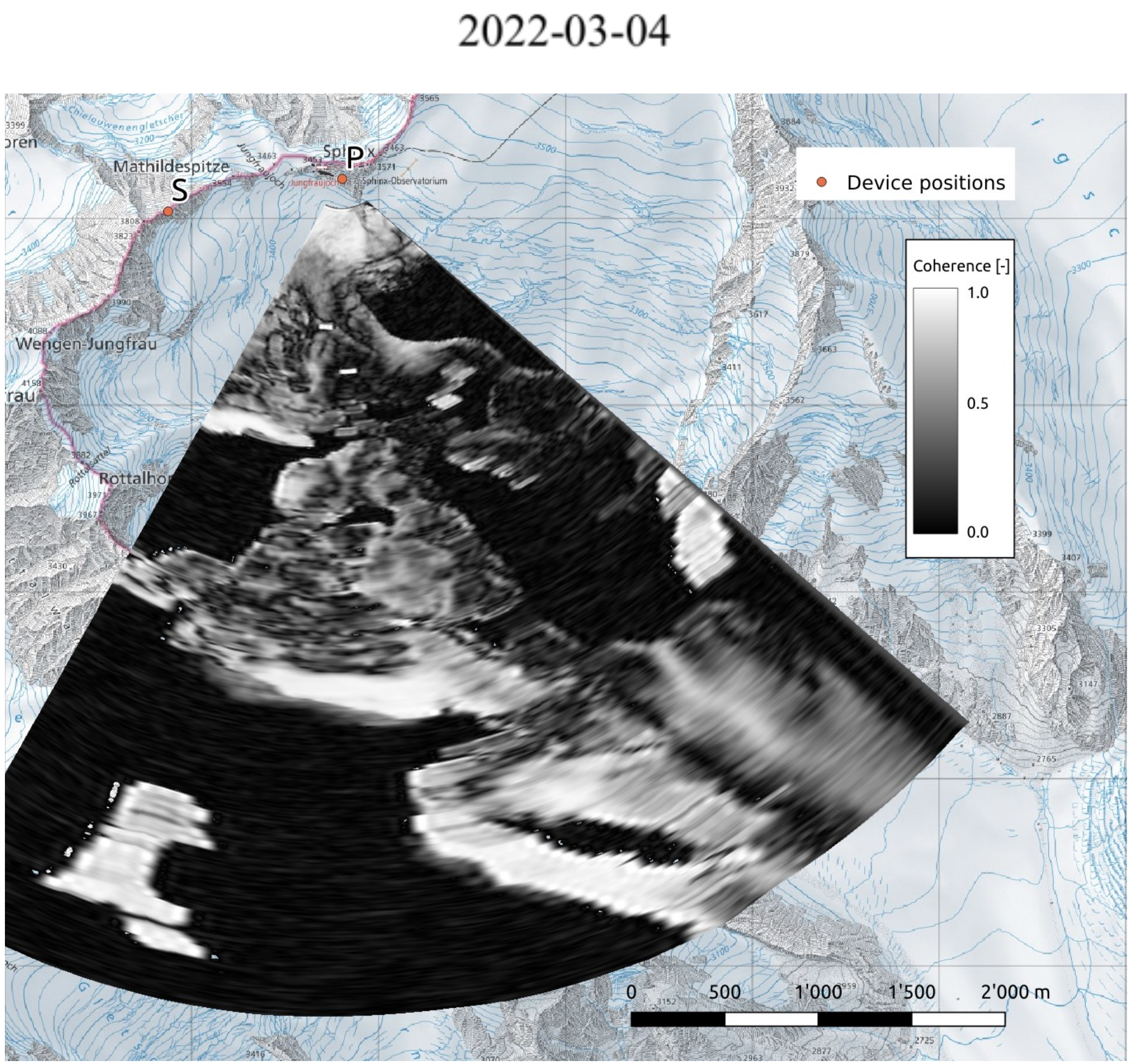

# KAPRI Synchronization

- Two options for oscillator synchronization:
  - Coaxial cable (a priori) <100m
  - Transmitted chirp (a posteriori) 100m – 2500m

$$s_{\mathrm{d}}(t) = \sigma^* e^{j2\pi\left(\left[\frac{p\gamma}{c}+\Delta f_c-\gamma'\Delta t\right]t+\frac{p}{\lambda}-\frac{p^2\gamma}{2c^2}+\frac{\Delta\gamma}{2}t^2-f_c'\Delta t+\frac{\gamma'}{2}\Delta t^2\right)}$$

$$s_{\mathrm{d-ref}}(t) = e^{j2\pi\left(\left[\frac{b\gamma}{c}+\Delta f_c-\gamma'\Delta t\right]t+\frac{b}{\lambda}-\frac{b^2\gamma}{2c^2}+\frac{\Delta\gamma}{2}t^2-f_c'\Delta t+\frac{\gamma'}{2}\Delta t^2\right)}$$

$$s_{\mathrm{d-corr}}(t) = s_d(t)s_{d-ref}(t)^* e^{j2\pi\frac{b\gamma}{c}t}$$

$$= \sigma^* e^{j2\pi\left(\frac{p\gamma}{c}t+\frac{p-b}{\lambda}-\frac{(p^2-b^2)\gamma}{2c^2}\right)}$$

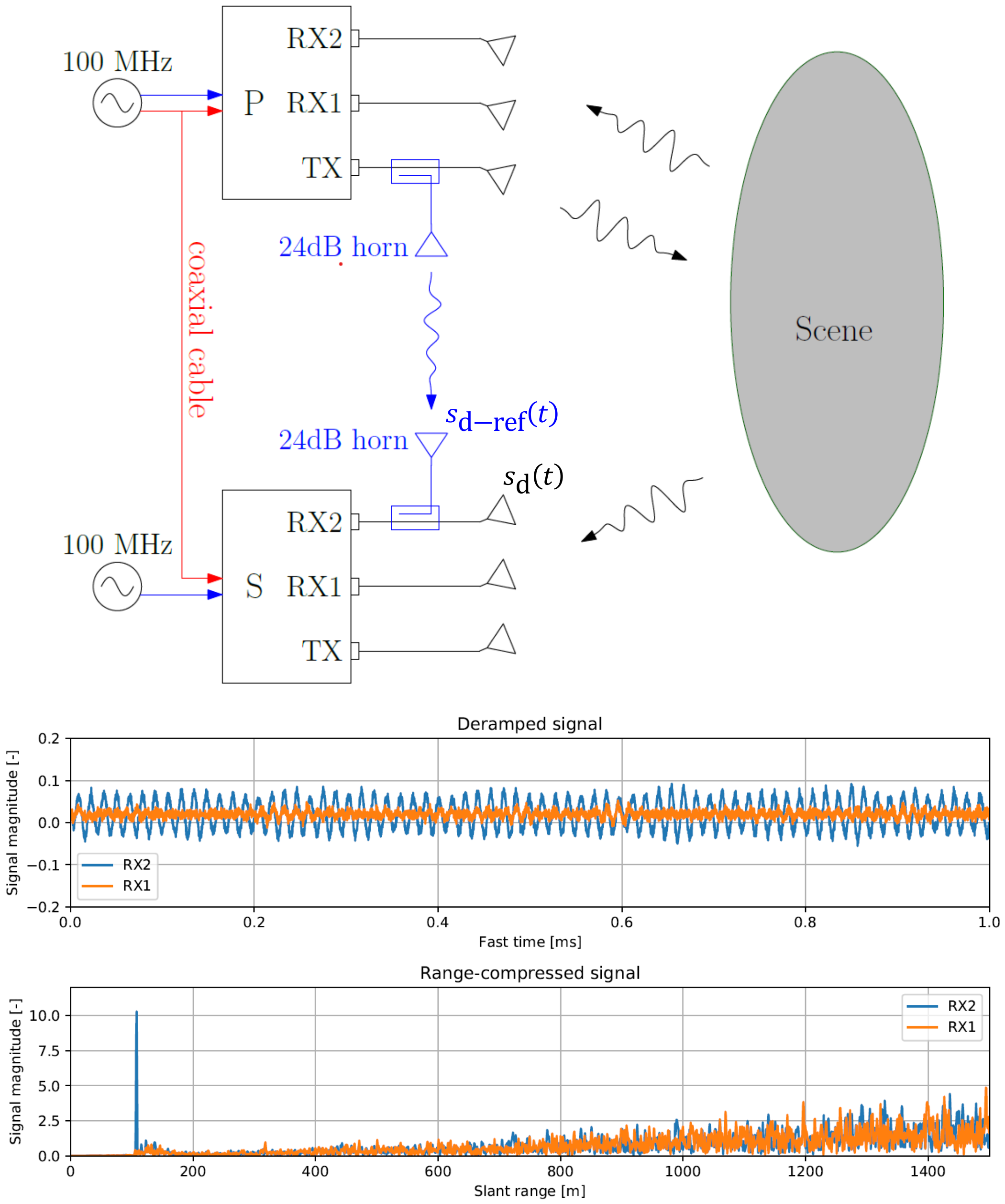

# Variable Signature Polarimetric Active Radar Calibrator (VSPARC)

- Requirements:
  - Quick field deployment
  - High radar cross-section independent of bistatic angle
  - Capable of responding in all polarimetric channels
- Solution:
  - Active calibrator
  - Antennas mounted on axial rotation stages enable variation of polarimetric response


$$\mathbf{S}_{\text{cal}} = e^{j\phi_{\text{abs}}(\varphi_T,\varphi_R)}\sqrt{G}\begin{bmatrix}\sin\varphi_T\sin\varphi_R & \cos\varphi_T\sin\varphi_R \\ \sin\varphi_T\cos\varphi_R & \cos\varphi_T\cos\varphi_R\end{bmatrix}$$

# Variable Signature Polarimetric Active Radar Calibrator (VSPARC)